Published in final edited form as:
J Med Chem. 2016 February 11; 59(3): 1140–1148. doi:10.1021/acs.jmedchem.5b01741.

Discovery of the First Potent and Selective Inhibitors of Human dCTP Pyrophosphatase 1

Sabin Llona-Minguez[#*,†,‡], **Andreas Höglund**[#†,⊥,‡], **Sylvain A. Jacques**[†,△], **Lars Johansson**[†,#], **José Manuel Calderón-Montaño**[†], **Magnus Claesson**[∞], **Olga Loseva**[†], **Nicholas C. K. Valerie**[†], **Thomas Lundbäck**[†,#], **Javier Piedrafita**[□], **Giovanni Maga**[§], **Emmanuele Crespan**[§], **Laurent Meijer**[‖], **Estefanía Burgos Morón**[†], **Pawel Baranczewski**[†,▽], **Ann-Louise Hagbjörk**[▽], **Richard Svensson**[▽], **Elisee Wiita**[†], **Ingrid Almlöf**[†], **Torkild Visnes**[†], **Fredrik Jeppsson**[†], **Kristmundur Sigmundsson**[†,#,○], **Annika Jenmalm Jensen**[†,#], **Per Artursson**[▽], **Ann-Sofie Jemth**[†], **Pål Stenmark**[∞], **Ulrika Warpman Berglund**[†], **Martin Scobie**[†], and **Thomas Helleday**[*,†]

[†]Division of Translational Medicine and Chemical Biology, Science for Life Laboratory, Department of Medical Biochemistry and Biophysics, Karolinska Institutet, Stockholm, Sweden

[#]Chemical Biology Consortium Sweden, Science for Life Laboratory, Division of Translational Medicine and Chemical Biology, Department of Medical Biochemistry and Biophysics, Karolinska Institutet, Stockholm, Sweden

[▽]Uppsala University Drug Optimization and Pharmaceutical Profiling Platform (UDOPP), Department of Pharmacy, Science for Life Laboratory, Uppsala University, Uppsala, Sweden

[∞]Department of Biochemistry and Biophysics, Stockholm University, Svante Arrhenius väg 16C, SE-106 91 Stockholm, Sweden

[§]Istituto di Genetica Molecolare, IGM-CNR, Via Abbiategrasso 207, 27100 Pavia, Italy

[‖]ManRos Therapeutics, Perharidy Research Center, 29680 Roscoff, Bretagne, France

[□]Torrey Pines Institute for Molecular Studies, 3550 General Atomics Court, San Diego, California 92121, United States

[#] These authors contributed equally to this work.

[*]Corresponding Authors: thomas.helleday@scilifelab.se; sabin.llona.minguez@scilifelab.se.
[⊥]Sprint BioScience AB, Huddinge, Sweden.
[△]LFCS, CAMB UMR7199 CNRS/LIT UMR7200 CNRS/Université de Strasbourg, MEDALIS Drug Discovery Center, Faculté de Pharmacie, 67401 Illkirch, France.
[○]Duke-NUS Graduate Medical School, Singapore.

[‡]**Author Contributions**

The manuscript was written through contributions of all authors. All authors have given approval to the final version of the manuscript.

The authors declare the following competing financial interest(s): A patent has been filed with data generated in this manuscript where S.L-M., T.H., A.H., S.A.J., M.S., and L.J. are listed as inventors.

ASSOCIATED CONTENT

Supporting Information

The Supporting Information is available free of charge on the ACS Publications website at DOI: 10.1021/acs.jmedchem.5b01741. Supplementary figures, additional data information regarding assays, and copies of ^{1}H and ^{13}C NMR spectra for relevant compounds (**14**, **18**, and **30**) (PDF)

Europe PMC Funders Author Manuscripts

Europe PMC Funders Author Manuscripts

Abstract

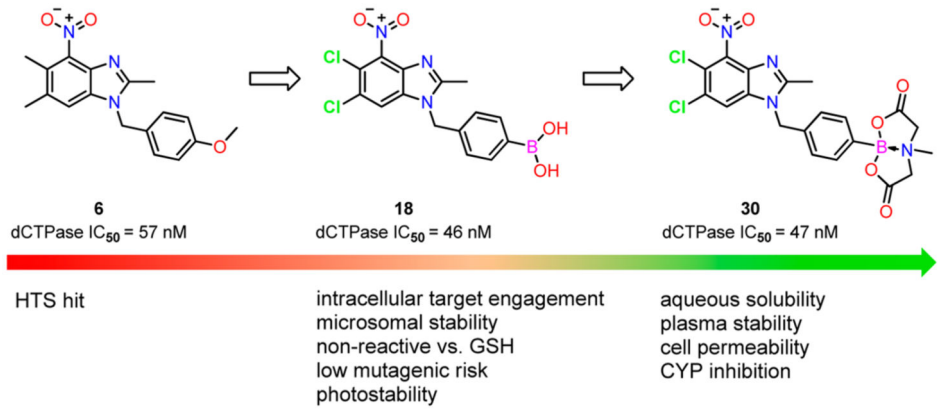

The dCTPase pyrophosphatase 1 (dCTPase) regulates the intracellular nucleotide pool through hydrolytic degradation of canonical and noncanonical nucleotide triphosphates (dNTPs). dCTPase is highly expressed in multiple carcinomas and is associated with cancer cell stemness. Here we report on the development of the first potent and selective dCTPase inhibitors that enhance the cytotoxic effect of cytidine analogues in leukemia cells. Boronate **30** displays a promising in vitro ADME profile, including plasma and mouse microsomal half-lives, aqueous solubility, cell permeability and CYP inhibition, deeming it a suitable compound for in vivo studies.

INTRODUCTION

dCTPase, also known as XTP3TPA, is an all-α nucleoside triphosphate (NTP) pyrophosphatase responsible for dNTP pool "house-cleaning".[1] More specifically, dCTPase catalyzes Mg^{2+}-mediated hydrolysis of dNTPs to the corresponding monophosphates, with higher affinity toward 5-modified noncanonical dNTPs over canonical dNTPs and rNTPs (5-I-dCTP > 5-formyl-dCTP > 5-Br-dCTP > 5-Me-dCTP > dCTP (**1**, Figure 1) ≫ CTP), leading to decreased intracellular levels of noncanonical dNTPs.[1,2] The dCTPase protein was originally identified in bacteria[3] and has recently been found to be overexpressed in multiple human carcinomas[4] and associated with cancer stemness.[2,5] Modulation of dNTP catabolism provides an exciting opportunity to regulate nucleotide homeostasis under pathologic conditions such as cancer and inflammation.[6-8] We have recently shown that inhibition of the dNTP pool-sanitizing enzyme MTH1 is an effective anticancer strategy: inhibition of MTH1 leads to increased incorporation of oxidized dNTPs in cancer cells, causing subsequent DNA damage and cell death in patient-derived xenografts.[9] Here we present a new case study of anticancer therapy exploiting the dNTP catabolic machinery. Cytidine analogues, such as decitabine (**2**, Figure 1), are currently used as first-line anticancer agents in myelodysplastic syndrome (MDS) and acute myeloid leukemia (AML). This class of drugs requires kinase-mediated phosphorylations to generate the corresponding triphosphates which are incorporated into DNA and/or RNA, where they exert their therapeutic effect. We hypothesized that some cytidine analogue triphosphates, such as 5-aza-dCTP (**3**, Figure 1), could act as noncanonical substrates of dCTPase given their structural resemblance to the enzyme's known substrates.[1] Inhibition of the dCTPase

enzyme should therefore suppress degradation of the drug's active triphosphate form and improve its anticancer effect.[10]

Despite the biological relevance of dCTPase, only a handful of weak non-drug-like dCTPase ligands have been identified using photo-cross-linking experiments (**4** and **5**, Figure 1).[11,12] In this article, we report on the discovery and development of a series of benzimidazole derivatives as the first potent and selective dCTPase inhibitors.

CHEMISTRY

The general synthesis of this series of benzimidazole derivatives is shown in Scheme 1. Ring formation of the heterocyclic core was accomplished by thermal heating of commercially available benzene-1,2-diamines in neat carboxylic acid.[13] Subsequent regioselective mononitration gave the corresponding 4-nitro-benzimidazoles in good yields,[14] followed by alkylation, arylation, sulfonylation, or acylation reactions to obtain the desired final products. Reactions were regioselective, and the corresponding 1,4-regioisomer products were formed almost exclusively, with only small amounts of the corresponding 1,7-regioisomers observed as alkylation side-products. *N*-Methyliminodiacetic acid (MIDA) boronate esters can be prepared from the parent boronic acids using Knapp's procedure.[15]

RESULTS AND DISCUSSION

To exploit the therapeutic potential of dCTPase inhibition, we purified the full-length human dCTPase protein and screened a proprietary compound collection (5.5K compounds, Chemical Biology Consortium Sweden at Karolinska Institutet). This was achieved using an HTS-adapted Malachite Green assay, a test for the colorimetric detection of inorganic phosphate (see Supporting Information).[16] The most potent hit from the screen was compound **6** (Table 1) which inhibited dCTPase activity by 98% at 10 μM and exhibited an IC_{50} value of 0.057 ± 0.02 μM, determined from three independent runs. Initially, we probed the importance of the substituents at the 2-, 4-, 5- and 6-positions of the benzimidazole core (Table 1). The methyl group at the benzimidazole 2-position appeared to be important for activity, as analogues lacking this substituent exhibited no inhibiton of dCTPase (compounds **7** and **8**). The importance of the 2-methyl group is further manifested when compound **7** (inactive) is compared to its 2-methyl analogue **10** (IC_{50} = 22 μM). However, the 2-methyl-substituted compound **9** showed no inhibition of dCTPase, demonstrating that the substituents in the 4-, 5-, and 6-positions of the benzimidazole ring are also important for the inhibitory properties. Interestingly, introduction of a nitro group at the 4-position led to a highly potent dCTPase inhibitor **6** and its replacement by hydrogen in **10** led to a dramatic 400 fold decrease in potency. On the other hand, when both the 5- and 6-methyl groups in **6** were replaced with hydrogens (compound **12**), the decrease in potency was approximately 25-fold. We were intrigued to find that the 5,6-dichloro analogue **11** was about twice as potent as the corresponding 5,6-dimethyl analogue **10**. For this reason, we next prepared a series of compounds based on the 4-nitro-5,6-dichlorobenzimidazole scaffold to investigate the SAR at the N1-substituent (Table 2). The unsubstituted benzyl analogue **13** and several para-substituted benzyl analogues (methoxy **14**, methyl **16**, boronic acid **18**, reversed methyl ester **21**, and the derived phenol **22**) were equipotent to compound **6**. Nitrile **15** and

carbonyl-containing derivatives (carboxylic acid **17**, methyl ester **19**, and aldehyde **20**) exhibited slightly decreased inhibitory activity, while heterocycle-containing analogues displayed even lower inhibition (compounds **23**, **24**, **25**, and **26**), with the exception of pyrazole **27**. Following up on the unusual boronic acid **18**, we determined that para was slightly preferred to ortho (**28**) substitution in the benzyl moiety and equipotent to meta (**29**) substitution, and boronic esters were tolerated as well (**30**) (Table 2). In a subsequent exploration we retained the active motifs present in compounds **6**, **13**, and **18** and explored close analogues to these by variations of the methylene chain connecting N1 and the aromatic ring (Table 3). Benzylic α-methylation (**33**) and linker extension (**32**) resulted in a significant drop in activity, whereas linker deletion (**31**) and sulfonamide (**34**) or carboxamide (**35**) replacements were less detrimental. Additional exploration of the 2-, 4-, 5-, and 6-positions of the benzimidazole ring (Table 4) indicated that other substituents other than 2-methyl were tolerated, for example 2-cyclopropyl (**36**) and 2-trifluoromethyl (**37**). When the benzyl boronic acid was present, compound **38** lacking the 4-nitro group retained submicromolar activity and so did the 5,6-difluoro analogue **39**.

Compounds **14** and **18** both showed a concentration-dependent stabilization of the purified dCTPase enzyme in a differential scanning fluorimetry assay (Supporting Information, Figure 1).[17] However, compound **14** did not stabilize dCTPase in a cellular thermal shift assay (Figure 2A),[18] possibly due to efflux issues, and suffered from high liver microsomal clearance (MLM/HLM $t_{1/2}$) (Table 5). Short MLM and/or HLM half-life was an issue often observed in this chemical series (see also analogues **25** and **27**). To our delight, the boronic acid analogue **18** enabled a strong intracellular target engagement (Figure 2A) and displayed enhanced microsomal stability and aqueous solubility (Table 5). Interestingly, replacement of the 2-methyl substituent in **18** with a cyclopropyl group in **36** improved stability in HLM but decreased in MLM (Table 5). Attracted by the chemical novelty of **18**, we decided to profile the compound in more depth. First, we investigated the nitro and boronic acid features of **18**. Although nitro aromatic compounds are often reported to be photoreactive,[19] a solution of **18** stored at room temperature under normal light conditions showed no signs of degradation over a period of five months (see Supporting Information). Then we investigated the in vitro reactivity of the electrophilic α-carbon to the nitro group. Compounds **18** and **30** did not conjugate with the endogenous nucleophile glutathione (GSH) in the presence of metabolic activation system (in HLM) (see Supporting Information). Next, we turned our attention to the boronic acid motif. Boron-containing drugs are uncommon and only a few compounds have reached the clinical stage in the fields of anti-infectives (tavaborole[20] and RPX7009[21]) and oncology (bortezomib[22] and delanzomib[23]) (see Supporting Information, Figure 2). Although boronic acid reagents are generally perceived as “low-toxicity” compounds, researchers at Lilly[24] and Astra Zeneca[25] have recently reported on the mutagenic potential of boronic acid derivatives. Given the potentially toxicity of also present nitro moiety,[26] we were pleased to observe that compound **18** did not increase DNA replication stress, as indicated by markers of single-strand (p-Chk1) and double-strand DNA breaks (γ-H2AX and 53BP1), nor cleaved caspase 3, indicative of apoptosis (Supporting Information, Figure 3), suggesting a low-mutagenic risk for **18** at the concentrations and time points tested. Because boronic acid-derived inhibitors can form covalent adducts with their biological targets,[27] we decided to further

characterize the dCTPase inhibition by **18** and **36** using a jump dilution assay.[28] Both inhibitors displayed a reversible off-rate at 10% of the IC_{50} concentration (90% activity of the control sample, see Supporting Information).

Given the encouraging profile of **18**, we decided to test the effect of the dCTPase inhibitor in HL60 leukemia cells, in combination with cytidine analogues of clinical relevance, such as 5-azacytidine (5aza), decitabine (5azadC), and gemcitabine (Supporting Information, Figure 6). Using the Chou–Talalay method for synergy quantification,[29] compound **18** showed a clear synergistic effect when combined with cytidine analogues increasing the cytotoxic action of the drugs against HL60 cells (Figure 2B). As expected, the combination treatment induced a concentration-dependent increase in cell death against the leukemia cells (Figure 2C).

Compounds **18** and **14** displayed excellent selectivity across a panel of related NTPases/NUDIX hydrolases (Supporting Information, Table 1) and other enzymes of pharmacological relevance, such as base excision repair enzymes (Supporting Information, Table 2), kinases (Supporting Information, Figure 4), and did not intercalate DNA (Supporting Information Figure 5). Unfortunately, **18** displayed only moderate aqueous solubility (52 μM), while suffering from low plasma stability (11% left after 4 h) and high plasma protein binding (F_u = 0.1%) (Table 5). This was most probably due to the presence of the boronic acid functionality (compare with phenol analogue **22**, Table 5). These suboptimal physicochemical and ADME properties limit the use of **18** to in vitro experiments. To develop a compound suitable for in vivo studies, we turned our attention to the *N*-methyliminodiacetic acid (MIDA) boronic acid derivative **30**. This chemical motif has gained popularity in recent years as a versatile building block for the synthesis of heteroaromatic compounds.[15,30] The MIDA boronate **30** inhibited dCTPase comparably to **18** (Table 2) and conferred enhanced aqueous solubility and improved plasma stability (Table 5). Compound **30** presented suitable in vitro $t_{1/2}$ in the presence of MLMs, but not HLMs, and an overall encouraging CYP inhibition profile, with only modest inhibition by CYP2C enzymes (Table 6), deeming it a suitable candidate for future studies in relevant MDS and AML mouse models.

CONCLUSIONS

Here we have described the discovery and subsequent medicinal chemistry optimization of the first potent and selective dCTPase inhibitors. This series of N1-substituted benzimidazole analogues relies on additional functionalities on the 2-, 4-, 5- and 6-positions of the heterocyclic core to achieve optimal inhibitory activity, although at least substitution at three out of those four positions is required for sub-micromolar dCTPase inhibition. Diverse aryl-containing substituents at the N1-position deliver compounds with nanomolar potency. Increased microsomal stability and intracellular target engagement was achieved thanks to the addition of a boronic acid functionality, as seen in compound **18**, which effectively synergized with cytidine analogues in killing HL60 leukemia cells. Despite its excellent selectivity profile and cellular efficacy, compound **18** lacked sufficient plasma stability required for in vivo studies. This issue was circumvented by masking the boronic acid functionality with a MIDA ester to deliver compound **30** with a suitable profile for

future experiments in murine leukemia models. Efforts to improve human microsomal stability on **30** are currently ongoing and will be reported in due course.

These results indicate that potent and selective dCTPase inhibitors can enhance the therapeutic effect of noncanonical cytidine analogues. Investigations to understand the biological relevance of dCTPase inhibition will provide invaluable insight into dNTP pool regulation and new potential applications for this type of therapeutic agents.

EXPERIMENTAL SECTION

Chemistry

All commercial reagents and solvents were used without further purification. Analytical thin-layer chromatography was performed on silica gel 60 F-254 plates (E. Merck) and visualized under a UV lamp. Flash column chromatography was performed in a Biotage SP4MPLC system using Merck silica gel 60 Å (40–63 mm mesh). ^{1}H NMR spectra were recorded on a Bruker DRX-400 and ^{13}C NMR spectra on a Bruker 600 MHz Avance III spectrometer. Chemical shifts are expressed in parts per million (ppm) and referenced to the residual solvent peak. Analytical HPLC-MS was performed on an Agilent MSD mass spectrometer connected to an Agilent 1100 system with method B1090A: column ACE 3 C8 (50 × 3.0 mm); H_2O (+ 0.1% TFA) and MeCN were used as mobile phases at a flow rate of 1 mL/min, with a gradient time of 3.0 min; or method 0597X3: column X-Terra MSC18 (50 × 3.0 mm); H_2O (containing 10 mM NH_4HCO_3; pH = 10) and MeCN were used as mobile phases at a flow rate of 1 mL/min, with a gradient time of 3.0 min. Preparative HPLC was performed on a Gilson HPLC system; basic pH: column Xbridge Prep C18, 5 μM CBD (30 × 75 mm); H_2O (containing 50 mM NH_4HCO_3; pH = 10) and MeCN were used as mobile phases at a flow rate of 45 mL/min, with a gradient time of 9 min. Acidic pH: column ACE 5 C8 (150 × 30 mm); H_2O (containing 0.1% TFA) and MeCN were used as mobile phases at a flow rate of 45 mL/min, with a gradient time of 9 min. For HPLC-MS, detection was made by UV using the 180–305 nM range and MS (ESI+). For preparative HPLC, detection was made by UV at 254 or 214 nM. All intermediates and final compounds were assessed to be >95% pure by HPLC-MS analysis, unless stated otherwise.

Method A

The appropriate aromatic diamine (2.0 mmol, 1.0 equiv) and carboxylic acid (10 equiv) were heated in a sealed tube at 145 °C for 20 min. The resulting solution was cooled to rt and then poured into a beaker containing ca. 10 mL of saturated Na_2CO_3. The precipitate was filtered off and triturated with water. The material was then dried in vacuo to afford the desired compound of general formula **I.1.X.**

1H-Benzo[d]imidazole (I-1.1), 5,6-dimethyl-1H-benzo[d]-imidazole (I-1.2) and 2-methyl-1H-benzo[d]imidazole (I-1.3)—Commercially available.

2,5,6-Trimethyl-1H-benzo[d]imidazole (I-1.4)—Yield 87%. Analytical data matching the literature report.[13]

5,6-Dichloro-2-methyl-1H-benzo[d]imidazole (I-1.5)—Reaction performed in 21 mmol scale. Yield 93%. Analytical data matching the literature report.[13]

2-Methyl-4-nitro-1H-benzo[d]imidazole (I-1.6)—Yield 84%. LCMS $[M + H]^+$ *m/z* 178. ^{1}H NMR (DMSO-d_6) *δ*: 13.00 (br s, 1 H), 8.05 (dd, *J* = 8.1, 0.9 Hz, 1 H), 7.98 (dd, *J* = 7.9 Hz, 0.9 Hz, 1 H), 7.33 (app t, *J* = 8.1 Hz, 1 H), 2.58 (s, 3 H)

5,6-Dichloro-2-cyclopropyl-1H-benzo[d]imidazole (I-1.7)—Yield 51%. LCMS $[M + H]^+$ *m/z* 227. ^{1}H NMR (DMSO-d_6) *δ*:12.62 (br s, 1 H), 7.66 (s, 2 H), 2.16–2.06 (m, 1 H), 1.12–1.05 (m, 2 H), 1.05–0.97 (m, 2 H)

4-Nitro-2-(trifluoromethyl)-1H-benzo[d]imidazole (I-1.8)—Yield 51%. LCMS $[M + H]^+$ *m/z* 232. ^{1}H NMR (DMSO-d_6) δ: 14.65 (br s, 1 H), 8.33 (d, *J* = 8.1 Hz, 1 H), 8.29 (d, *J* = 7.3 Hz, 1 H), 7.59 (t, *J* = 8.1 Hz, 1 H)

4-Nitro-2-(trifluoromethyl)-1H-benzo[d]imidazole (I-1.9)—Yield 68%. Analytical data matching the literature report.[13]

Method B

A 65% HNO_3 (1.1 equiv) solution was added dropwise to an appropriately substituted heteroaryl compound of general formula **I-1.X** (1.0 mmol, 1.1 equiv) in a mixture of MTBE/MeCN (2:1, 0.4 M) at 0 °C. The mixture was stirred at 0 °C for 1 h after which the reaction was concentrated in vacuo. The residue was suspended in DCM (0.4 M), and the mixture was added dropwise to ice-cold 95% H_2SO_4 (10 equiv). The mixture was allowed to warm to rt and stirred for 16 h. The mixture was poured onto ice—water and neutralized with concd NH_4OH while keeping the temperature below 5 °C. The mixture was filtered and dried to afford the desired compound of general formula **I-2.X**.

2,5,6-Trimethyl-4-nitro-1H-benzo[d]imidazole (I-2.1)—Yield 85%. LCMS $[M + H]^+$ *m/z* 206. ^{1}H NMR (DMSO-d_6) *δ*: 12.56 (br s, 1 H), 7.73 (s, 0.4H, minor tautomer), 7.47 (s, 0.6H, major tautomer), 2.47–2.49 (m, 4.2 H), 2.40 (s, 1.2H, minor tautomer), 2.38 (s, 1.8H, major tautomer), 2.21 (s, 1.8H, major tautomer)

5,6-Dichloro-2-methyl-4-nitro-1H-benzo[d]imidazole (I-2.2)—Reaction performed in 24 mmol scale. Yield 86%. LCMS $[M + H]^+$ *m/z* 246. ^{1}H NMR (DMSO-d_6) *δ*: 13.14 (br s, 1 H), 8.10 (s, 1 H), 2.56 (s, 3 H)

5,6-Dichloro-2-cyclopropyl-4-nitro-1H-benzo[d]imidazole (I-2.3)—Yield 49%. LCMS $[M + H]^+$ *m/z* 272. ^{1}H NMR ($CDCl_3$) *δ*: 10.13 (br s, 1 H), 7.99 (s, 1 H), 2.10 (m, 1 H), 1.28 (m, 4H)

Method C1. When R^1 = Arylalkyl

A mixture of the appropriate alkyl halide (1.5 equiv), the appropriate heteroaromatic intermediate of general formula **1.2.X** or **2.X** (0.1 mmol, 1.0 equiv), K_2CO_3 (2 equiv), and DMSO (0.2 M) was stirred at rt for 16 h (for reactions using an alkyl chloride as the

alkylating agent, one crystal of potassium iodide was added to the reaction mixture). The mixture was purified by preparative HPLC basic pH to afford the desired compound.

1-(4-Methoxybenzyl)-2,5,6-trimethyl-4-nitro-1H-benzo[d]-imidazole (6)—Yield 87%. LCMS $[M + H]^+$ *m/z* 326. ^{1}H NMR (DMSO-d_6) *δ*: 7.63 (s, 1 H), 7.09 (m, 2 H), 6.89 (m, 2 H), 6.58 (m, 2 H), 5.41 (s, 2 H), 3.70 (s, 3 H), 2.51 (s, 3 H), 2.37 (s, 3 H), 2.22 (s, 3 H)

1-(4-Methoxybenzyl)-1H-benzo[d]imidazole (7)—Yield 53%. LCMS $[M + H]^+$ *m/z* 239. ^{1}H NMR (DMSO-d_6) *δ*: 8.38 (s, 1 H), 7.63 (m, 1 H), 7.52 (m, 1 H), 7.28 (m, 2 H), 7.19 (m, 2 H), 6.88 (m, 2 H), 5.40 (s, 2 H), 3.70 (s, 3 H)

1-(4-Methoxybenzyl)-5,6-dimethyl-1H-benzo[d]imidazole (8)—Yield 53%. LCMS $[M + H]^+$ *m/z* 267. ^{1}H NMR (DMSO-d_6) *δ*: 8.21 (s, 1 H), 7.40 (s, 1 H), 7.29 (s, 1 H), 7.23 (m, 2 H), 6.88 (m, 2 H), 5.34 (s, 2 H), 3.70 (s, 3 H), 2.27 (s, 6 H)

1-(4-Methoxybenzyl)-2-methyl-1H-benzo[d]imidazole (9)—Yield 51%. LCMS $[M + H]^+$ *m/z* 253. ^{1}H NMR (DMSO-d_6) *δ*: 7.52 (m, 1 H), 7.47 (m, 1 H), 7.13 (m, 2 H), 7.09 (m 2 H), 6.88 (m, 2 H), 5.38 (s, 2 H), 3.70 (s, 3 H), 2.52 (s, 3 H)

1-(4-Methoxybenzyl)-2,5,6-trimethyl-1H-benzo[d]imidazole (10)—Yield 29%. LCMS $[M + H]^+$ *m/z* 281. ^{1}H NMR (DMSO-d_6) *δ*: 7.30 (s 1 H), 7.23 (s, 1 H), 7.04 (m, 2 H), 6.87 (m, 2 H), 5.30 (s 2 H), 3.70 (s, 3 H), 2.45 (s, 3 H), 2.27 (s, 6 H)

5,6-Dichloro-1-(4-methoxybenzyl)-2-methyl-1H-benzo[d]-imidazole (11)—Yield 56%. LCMS $[M + H]^+$ *m/z* 321. ^{1}H NMR (DMSO-d_6) *δ*: 7.90 (s, 1 H), 7.80 (s, 1 H), 7.10 (m, 2 H), 6.89 (m, 2 H), 5.41 (s, 2 H), 3.70 (s, 3 H), 2.52 (s, 3 H)

1-(4-Methoxybenzyl)-2-methyl-4-nitro-1H-benzo[d]imidazole (12)—Yield 55%. LCMS $[M + H]^+$ *m/z* 298. ^{1}H NMR (DMSO-d_6) *δ*: 7.99 (dd, *J* = 8.0, 0.9 Hz, 1 H), 7.98 (dd, *J* = 8.1, 0.9 Hz, 1 H), 7.36 (app t, *J* = 8.1 Hz, 1 H), 7.12 (m, 2 H), 6.89 (m, 2 H), 5.51 (s, 2 H), 3.70 (s, 3 H), 2.64 (s, 3 H)

1-Benzyl-5,6-dichloro-2-methyl-4-nitro-1H-benzo[d]imidazole (13)—Yield 73%. LCMS $[M + H]^+$ *m/z* 336. ^{1}H NMR (DMSO-d_6) *δ*: 8.31 (s, 1 H), 7.35 (m, 3 H), 7.16 (m, 2 H), 5.59 (s, 2 H), 2.55 (s, 3 H)

5,6-Dichloro-1-(4-methoxybenzyl)-2-methyl-4-nitro-1H-benzo-[d]imidazole (14)—Yield 74%. LCMS $[M + H]^+$ *m/z* 366. ^{1}H NMR (DMSO-d_6) *δ*: 8.32 (s, 1 H), 7.15 (app d, *J* = 8.3 Hz, 2 H), 6.90 (app d, *J* = 8.4 Hz, 2 H), 5.50 (s, 2 H), 3.71 (s, 3 H), 2.57 (s, 3 H). ^{13}C NMR (DMSO-d_6) *δ*: 158.9 (C), 157.9 (C), 138.7 (C), 136.2 (C), 134.0 (C), 128.5 (CH), 127.6 (C), 124.8 (C), 115.3 (C), 114.6 (CH), 114.3 (CH), 55.1 (CH_3), 46.5 (CH_2), 14.0 (CH_3)

4-((5,6-Dichloro-2-methyl-4-nitro-1H-benzo[d]imidazol-1-yl)-methyl)benzonitrile (15)—Yield 61%. LCMS $[M + H]^+$ *m/z* 361. ^{1}H NMR (DMSO-d_6)

δ: 8.31 (s, 1 H), 7.78–7.85 (app d, *J* = 8.3 Hz, 2 H), 7.28–7.34 (app d, *J* = 8.3 Hz, 2 H), 5.71 (s, 2 H), 2.53 (s, 3 H)

5,6-Dichloro-2-methyl-1-(4-methylbenzyl)-4-nitro-1H-benzo[d]-imidazole (16)— Yield 57%. LCMS $[M + H]^+$ *m/z* 350. ^{1}H NMR (DMSO-d_6) *δ*: 8.30 (s, 1 H), 7.16 (m, 2 H), 7.06 (m, 2 H), 5.53 (s, 2 H), 2.55 (s, 3 H), 2.26 (s, 3 H)

4-((5,6-Dichloro-2-methyl-4-nitro-1H-benzo[d]imidazol-1-yl)-methyl)benzoic Acid (17)—Purified by preparative HPLC (acidic pH). Yield 50%. LCMS $[M + H]^+$ *m/z* 380. ^{1}H NMR (DMSO-d_6) *δ*: 12.98 (br s, 1 H), 8.31 (s, 1 H), 7.94–7.89 (app d, *J* = 8.3 Hz, 2 H), 7.28–7.21 (app d, *J* = 8.3 Hz, 2 H), 5.68 (s, 2 H), 2.53 (s, 3 H)

(4-((5,6-Dichloro-2-methyl-4-nitro-1H-benzo[d]imidazol-1-yl)-methyl)phenyl)boronic Acid (18)—Yield 67%. LCMS $[M + H]^+$ *m/z* 380. ^{1}H NMR (DMSO-d_6) *δ*: 8.29 (s, 1 H), 8.06 (s, 2 H), 7.75 (app d, *J* = 8.1 Hz, 2 H), 7.10 (app d, *J* = 8.1 Hz, 2 H), 5.59 (s, 2 H), 2.54 (s, 3 H). ^{13}C NMR (DMSO-d_6) *δ*: 158.0 (C), 138.7 (C), 137.4 (C), 136.4 (C), 134.7 (2 × CH), 134.0 (C), 125.8 (2 × CH), 124.9 (C), 115.4 (C), 114.6 (CH), 47.0 (CH_2), 13.9 (CH_3)

Methyl 4-((5,6-Dichloro-2-methyl-4-nitro-1H-benzo[d]imidazol-1-yl)methyl)benzoate (19)—Yield 61%. LCMS $[M + H]^+$ *m/z* 394. ^{1}H NMR ($CDCl_3$) *δ*: 8.03 (app d, *J* = 8.3 Hz, 2 H), 7.43 (s, 1 H), 7.08 (app d, *J* = 8.3 Hz, 2 H), 5.38 (s, 2 H), 3.92 (s, 3 H), 2.61 (s, 3 H)

4-((5,6-Dichloro-2-methyl-4-nitro-1H-benzo[d]imidazol-1-yl)-methyl)benzaldehyde (20)—Reaction performed in acetone. Purified by FCC (5–75% EtOAc in hexanes). Yield 57%. LCMS $[M + H]^+$ *m/z* 364. ^{1}H NMR ($CDCl_3$) *δ*: 10.01 (s, 1 H), 7.89 (app d, *J* = 8.03 Hz, 2 H), 7.43 (s, 1 H), 7.18 (app d, *J* = 8.03 Hz, 2 H), 5.41 (s, 2 H), 2.62 (s, 3 H)

4-((5,6-Dichloro-2-methyl-4-nitro-1H-benzo[d]imidazol-1-yl)-methyl)phenyl Acetate (21)—Reaction performed in acetone. Yield 46%. LCMS $[M + H]^+$ *m/z* 394. ^{1}H NMR ($CDCl_3$) *δ*: 7.46 (s, 1 H), 7.12–7.07 (m, 2 H), 7.05–7.00 (m, 2 H), 5.32 (s, 2 H), 2.62 (s, 3 H), 2.30 (s, 3 H)

4-((5,6-Dichloro-2-methyl-4-nitro-1H-benzo[d]imidazol-1-yl)-methyl)-2-methylthiazole (23)—Reaction performed in acetone. Purified by FCC (1–15% EtOAc in hexanes). Yield 29%. LCMS $[M + H]^+$ *m/z* 394. ^{1}H NMR ($CDCl_3$) *δ*: 7.64 (s, 1 H), 6.83 (s, 1 H), 5.34 (s, 2 H), 2.74 (s, 3 H), 2.67 (s, 3 H)

5,6-Dichloro-1-((6-chloropyridin-3-yl)methyl)-2-methyl-4-nitro-1H-benzo[d]imidazole (24)—Reaction performed in acetone. Purified by FCC (5–75% EtOAc in hexanes). Yield 15%. LCMS $[M + H]^+$ *m/z* 371. ^{1}H NMR ($CDCl_3$) *δ*: 8.30 (d, *J* = 2.3 Hz, 1 H), 7.45 (s, 1 H), 7.33 (d, *J* = 8.0 Hz, 1 H), 7.21 (dd, *J* = 2.3, 8.0 Hz, 1 H), 5.34 (s, 2 H), 2.64 (s, 3 H)

5,6-Dichloro-1-(2-(3,5-dimethyl-1H-pyrazol-4-yl)ethyl)-2-methyl-4-nitro-1H-benzo[d]imidazole (25)—Yield 13%. LCMS $[M + H]^+$ *m/z* 368. ^{1}H NMR (DMSO-d_6) *δ*: 11.92 (br s, 1 H), 8.01 (s, 1 H), 4.34 (t, *J* = 6.2 Hz, 1 H), 2.73 (t, *J* = 6.2 Hz, 2 H), 2.23 (s, 3 H), 1.55–1.85 (br s, 6H)

1-(4-(1H-Pyrrol-1-yl)benzyl)-5,6-dichloro-2-methyl-4-nitro-1H-benzo[d]imidazole (26)—Yield 25%. LCMS $[M + H]^+$ *m/z* 401. ^{1}H NMR (DMSO-d_6) *δ*: 8.33 (s, 1 H), 7.50–7.56 (m, 2 H), 7.40 (app t, *J* = 7.8 Hz, 1 H), 7.35 (app t, *J* = 2.2 Hz, 2 H), 6.89 (app d, *J* = 7.5 Hz, 1 H), 6.27 (app t, *J* = 2.2 Hz, 2 H), 5.62 (s, 2 H), 4.07–4.49 (m, 1 H), 2.59 (s, 3 H)

1-(4-(1H-Pyrazol-1-yl)benzyl)-5,6-dichloro-2-methyl-4-nitro-1H-benzo[d]imidazole (27)—Yield 10%. LCMS $[M + H]^+$ *m/z* 402. ^{1}H NMR ($CDCl_3$) *δ*: 7.90 (app d, *J* = 2.5 Hz, 1 H), 7.68–7.73 (m, 3 H), 7.46 (app s, 1 H), 7.12 (d, *J* = 8.8 Hz, 2 H), 6.45–6.50 (m, 1 H), 5.35 (s, 2 H), 2.63 (s, 3 H)

(3-((5,6-Dichloro-2-methyl-4-nitro-1H-benzo[d]imidazol-1-yl)-methyl)phenyl)boronic Acid (28)—Purified by preparative HPLC (acidic pH). Yield 43%. LCMS $[M + H]^+$ *m/z* 380. ^{1}H NMR (CD_3OD) *δ*: 7.93 (s, 1 H), 7.57–7.54 (m, 1 H), 7.43–7.31 (m, 2 H), 7.16–7.14 (m, 1 H), 5.53 (s, 2 H), 2.60 (s, 3 H)

(2-((5,6-Dichloro-2-methyl-4-nitro-1H-benzo[d]imidazol-1-yl)-methyl)phenyl)boronic Acid (29)—Purified by preparative HPLC (acidic pH). Yield 49%. LCMS $[M + H]^+$ *m/z* 380. ^{1}H NMR (CD_3OD) *δ*: 7.74 (s, 1 H), 7.45–7.39 (m, 1 H), 7.39–7.34 (m, 2 H), 7.10–7.05 (m, 1 H), 5.52 (s, 2 H), 2.55 (s, 3 H)

(4-((5,6-Dichloro-2-cyclopropyl-4-nitro-1H-benzo[d]imidazol-1-yl)methyl)phenyl)boronic Acid (36)—Purified by preparative HPLC (acidic pH). Yield 48%. LCMS $[M + H]^+$ *m/z* 406. ^{1}H NMR (acetone-d_6) *δ*: 8.01 (s, 1 H), 7.85–7.89 (m, 2 H), 7.24–7.27 (m, 2 H), 5.77 (s, 2 H), 2.27–2.31 (m, 1 H), 1.14–1.19 (m, 4H)

(4-((4-Nitro-2-(trifluoromethyl)-1H-benzo[d]imidazol-1-yl)-methyl)phenyl)boronic Acid (37)—Yield 58%. LCMS $[M + H]^+$ *m/z* 366. ^{1}H NMR (CD_3OD) *δ*: 8.26–8.20 (m, 1 H), 7.94–7.92 (m, 1 H), 7.70 (br s, 1 H), 7.60 (br s, 1 H), 7.60–7.55 (m, 1 H), 7.10–7.05 (m, 2 H), 5.78 (s, 2 H)

(4-((5,6-Dichloro-2-methyl-1H-benzo[d]imidazol-1-yl)methyl)-phenyl)boronic Acid (38)—Yield 42%. LCMS $[M + H]^+$ *m/z* 335. ^{1}H NMR (CD_3OD) *δ*: 7.71 (s, 1 H), 7.65–7.55 (m, 3 H), 7.08 (app d, *J* = 6.6 Hz, 2 H), 5.45 (s, 2 H), 2.55 (s, 3 H)

(4-((5,6-Difluoro-2-methyl-4-nitro-1H-benzo[d]imidazol-1-yl)-methyl)phenyl)boronic Acid (39)—Yield 76%. LCMS $[M + H]^+$ *m/z* 348. ^{1}H NMR (CD_3OD) *δ*: 7.91–8.01 (m, 1 H), 7.74–7.62 (m, 2 H), 7.19–7.08 (m, 2 H), 5.60 (s., 2 H), 2.72 (s, 3 H)

Method C2

5,6-Dichloro-2-methyl-4-nitro-1-phenyl-1H-benzo-[d]imidazole (31)—A mixture of **I-2.2** (1.0 equiv), phenyl boronic acid (0.1 mmol, 1.0 equiv), copper acetate (1.0 equiv), pyridine (2.0 equiv), and DCM (0.1 M) was stirred at rt for 4 days. The mixture was cooled and purified by FCC (5–30% EtOAc in hexanes) to afford **31**. Yield 15%. LCMS $[M + H]^+$ *m/z* 322. ^{1}H NMR ($CDCl_3$) *δ*: 7.60–7.69 (m, 3 H), 7.36 (s, 1 H), 7.32–7.36 (m, 2 H), 2.54 (s, 3 H)

Method C3

5,6-Dichloro-2-methyl-4-nitro-1-(phenylsulfonyl)-1H-benzo[d]imidazole (32)—A mixture of **I-2.2** (0.1 mmol, 1.0 equiv), benzenesulfonyl chloride (1.5 equiv), triethylamine (1.0 equiv), and DCM (0.1 M) was stirred at rt for 16 h. The mixture was cooled and purified by FCC (20% EtOAc in hexanes) to afford **32**. Yield 64%. LCMS $[M + H]^+$ *m/z* 322. ^{1}H NMR ($CDCl_3$) *δ*: 8.36 (s, 1 H), 7.95–7.90 (m, 2 H), 7.77–7.71 (m, 1 H), 7.64–7.57 (m, 2 H), 2.81 (s, 3 H)

Method C4

5,6-Dichloro-2-methyl-4-nitro-1H-benzo[d]-imidazol-1-yl) (phenyl)methanone (33)—A mixture of **I-2.2** (1.0 equiv), benzoyl chloride (1.5 equiv), triethylamine (1.0 equiv), and DCM (0.1 M) was stirred at rt for 16 h. The mixture was cooled and purified by FCC (20% EtOAc in hexanes) to afford **33**. Yield 73%. LCMS $[M + H]^+$ *m/z* 350. ^{1}H NMR ($CDCl_3$) *δ*: 7.82–7.72 (m, 3 H), 7.64–7.58 (m, 2 H), 7.28 (s, 1 H), 2.65 (s, 3 H)

Method D

4-((5,6-Dichloro-2-methyl-4-nitro-1H-benzo[d]-imidazol-1-yl)methyl)phenol (22)—A solution of LiOH (1.5 equiv) in water (1 M) was added to carboxylic ester **21** (0.1 mmol, 1.0 equiv) in 1,4-dioxane (0.06 M) at rt. The mixture was stirred at rt for 16 h and purified by preparative HPLC basic pH to afford phenol **22**. Yield 86%. LCMS $[M + H]^+$ *m/z* 352. ^{1}H NMR (DMSO-d_6) *δ*: 9.48 (s, 1 H), 8.29 (s, 1 H), 7.08–6.99 (m, 2 H), 6.76–6.66 (m, 2 H), 5.44 (s, 2 H), 2.56 (s, 3 H)

Method E

2-(4-((5,6-Dichloro-2-methyl-4-nitro-1H-benzo[d]-imidazol-1-yl)methyl)phenyl)-6-methyl-1,3,6,2-dioxazaborocane-4,8-dione (30)—A mixture of **18** (0.1 mmol, 1.0 equiv), *N*-methyliminodiacetic acid (1.5 equiv), $MgSO_4$ (10 equiv), and toluene/DMSO (9:1, 0.05 M) was refluxed for 1 h. The mixture was cooled and purified by FCC (0–60% diethyl ether in MeCN) to afford **30**. Yield 89%. LCMS $[M + H]^+$ *m/z* 491. ^{1}H NMR (DMSO-d_6) *δ*: 8.30 (s, 1 H), 7.46–7.37 (m, *J* = 8.1 Hz, 2 H), 7.20–7.12 (m, *J* = 8.1 Hz, 2 H), 5.60 (s, 2 H), 4.31 (d, *J* = 17.4 Hz, 2 H), 4.08 (d, *J* = 17.1 Hz, 2 H), 2.54 (s, 3 H), 2.46 (s, 3 H). ^{13}C NMR (DMSO-d_6) *δ*:169.3, 158.0, 138.7, 136.4, 136.3, 134.0, 133.0, 126.2, 124.9, 115.3, 114.6, 61.7, 47.5, 47.0, 14.0.

Supplementary Material

Refer to Web version on PubMed Central for supplementary material.

ACKNOWLEDGMENTS

This project is primarily supported by The Knut and Alice Wallenberg Foundation. Further support was received from the Felix Mindus foundation for leukemia research (A.H.), the Swiss National Science Foundation (F.G.), the Swedish Research Council (T.H., A.JJ., P.S.), the European Research Council (T.H.), Göran Gustafsson Foundation (T.H.), Swedish Cancer Society (T.H., P.S.), the Swedish Children's Cancer Foundation (T.H.), the Swedish Pain Relief Foundation (T.H.), Carl Tryggers Foundation (P.S.), Wenner-Gren Foundation (P.S), and the Torsten and Ragnar Söderberg Foundation (T.H.). Chemical Biology Consortium Sweden was supported by the Swedish Research Council. We also acknowledge ChemAxon (http://www.chemaxon.com) for technical support. We are grateful to Hans Krokan at Norwegian University of Science and Technology and Susan Wallace at University of Vermont for donation of plasmid materials and to the Protein Science Facility at Karolinska Institutet for purification of proteins.

ABBREVIATIONS USED

XTP3TPA	XTP3-transactivated protein A
NTP	nucleoside triphosphate
dNTP	deoxynucleoside triphosphate
rNTP	ribonucleoside triphosphate
HTS	high throughput screen
DSF	differential scanning fluorimetry
MLM	mouse liver microsomes
HLM	human liver microsomes
CYP	cytochrome
FCC	flash column chromatography
E	extraction ratio
$\boldsymbol{P_{app}}$	apparent permeability coefficient

REFERENCES

(1). Requena CE, Perez-Moreno G, Ruiz-Perez LM, Vidal AE, Gonzalez-Pacanowska D. The NTP pyrophosphatase DCTPP1 contributes to the homoeostasis and cleansing of the dNTP pool in human cells. Biochem. J. 2014; 459:171–180. [PubMed: 24467396]

(2). Song FF, Xia LL, Ji P, Tang YB, Huang ZM, Zhu L, Zhang J, Wang JQ, Zhao GP, Ge HL, Zhang Y, Wang Y. Human dCTP pyrophosphatase 1 promotes breast cancer cell growth and stemness through the modulation on 5-methyl-dCTP metabolism and global hypomethylation. Oncogenesis. 2015; 4:e159. [PubMed: 26075750]

(3). Koerner JF, Smith MS, Buchanan JM. A deoxycytidine triphosphate splitting enzyme and the synthesis of the deoxyribose-nucleic acid of T2 bacteriophage 1. J. Am. Chem. Soc. 1959; 81:2594–2595.

(4). Zhang Y, Ye WY, Wang JQ, Wang SJ, Ji P, Zhou GY, Zhao GP, Ge HL, Wang Y. dCTP pyrophosphohydrase exhibits nucleic accumulation in multiple carcinomas. Eur. J. Histochem. 2013; 57:e29. [PubMed: 24085278]

(5). Morisaki T, Yashiro M, Kakehashi A, Inagaki A, Kinoshita H, Fukuoka T, Kasashima H, Masuda G, Sakurai K, Kubo N, Muguruma K, Ohira M, Wanibuchi H, Hirakawa K. Comparative proteomics analysis of gastric cancer stem cells. PLoS One. 2014; 9:e110736/1–e110736/16. [PubMed: 25379943]

(6). Henderson JP, Byun J, Williams MV, McCormick ML, Parks WC, Ridnour LA, Heinecke JW. Bromination of deoxycytidine by eosinophil peroxidase: A mechanism for mutagenesis by oxidative damage of nucleotide precursors. Proc. Natl. Acad. Sci. U. S. A. 2001; 98:1631–1636. [PubMed: 11172002]

(7). Henderson JP, Byun J, Williams MV, Mueller DM, McCormick ML, Heinecke JW. Production of brominating intermediates by myeloperoxidase: a transhalogenation pathway for generating mutagenic nucleobases during inflammation. J. Biol. Chem. 2001; 276:7867–7875. [PubMed: 11096071]

(8). Valinluck V, Wu W, Liu P, Neidigh JW, Sowers LC. Impact of Cytosine 5-Halogens on the Interaction of DNA with Restriction Endonucleases and Methyltransferase. Chem. Res. Toxicol. 2006; 19:556–562. [PubMed: 16608167]

(9). Gad H, Koolmeister T, Jemth A-S, Eshtad S, Jacques SA, Strom CE, Svensson LM, Schultz N, Lundback T, Einarsdottir BO, Saleh A, Gokturk C, Baranczewski P, Svensson R, Berntsson RPA, Gustafsson R, Stromberg K, Sanjiv K, Jacques-Cordonnier M-C, Desroses M, Gustavsson A-L, Olofsson R, Johansson F, Homan EJ, Loseva O, Brautigam L, Johansson L, Hoglund A, Hagenkort A, Pham T, Altun M, Gaugaz FZ, Vikingsson S, Evers B, Henriksson M, Vallin KSA, Wallner OA, Hammarstrom LGJ, Wiita E, Almlof I, Kalderen C, Axelsson H, Djureinovic T, Puigvert JC, Haggblad M, Jeppsson F, Martens U, Lundin C, Lundgren B, Granelli I, Jensen AJ, Artursson P, Nilsson JA, Stenmark P, Scobie M, Berglund UW, Helleday T. MTH1 inhibition eradicates cancer by preventing sanitation of the dNTP pool. Nature. 2014; 508:215–221. [PubMed: 24695224]

(10). Jansen R, Rosing H, Wijermans P, Keizer R, Schellens JM, Beijnen J. Decitabine triphosphate levels in peripheral blood mononuclear cells from patients receiving prolonged low-dose decitabine administration: a pilot study. Cancer Chemother. Pharmacol. 2012; 69:1457–1466. [PubMed: 22382880]

(11). Corson TW, Cavga H, Aberle N, Crews CM. Triptolide Directly Inhibits dCTP Pyrophosphatase. ChemBioChem. 2011; 12:1767–1773. [PubMed: 21671327]

(12). Kambe T, Correia BE, Niphakis MJ, Cravatt BF. Mapping the Protein Interaction Landscape for Fully Functionalized Small-Molecule Probes in Human Cells. J. Am. Chem. Soc. 2014; 136:10777–10782. [PubMed: 25045785]

(13). Treu M, Karner T, Kousek R, Berger H, Mayer M, McConnell DB, Stadler A. Microwave-Assisted Parallel Synthesis of Fused Heterocycles in a Novel Parallel Multimode Reactor. J. Comb. Chem. 2008; 10:863–868. [PubMed: 18808188]

(14). Zhang P, Cedilote M, Cleary TP, Pierce ME. Mononitration of aromatic compounds via their nitric acid salts. Tetrahedron Lett. 2007; 48:8659–8664.

(15). Knapp DM, Gillis EP, Burke MD. A General Solution for Unstable Boronic Acids: Slow-Release Cross-Coupling from Air-Stable MIDA Boronates. J. Am. Chem. Soc. 2009; 131:6961–6963. [PubMed: 19405470]

(16). Itaya K, Ui M. A new micromethod for the colorimetric determination of inorganic phosphate. Clin. Chim. Acta. 1966; 14:361–366. [PubMed: 5970965]

(17). Lo M-C, Aulabaugh A, Jin G, Cowling R, Bard J, Malamas M, Ellestad G. Evaluation of fluorescence-based thermal shift assays for hit identification in drug discovery. Anal. Biochem. 2004; 332:153–159. [PubMed: 15301960]

(18). Molina DM, Jafari R, Ignatushchenko M, Seki T, Larsson EA, Dan C, Sreekumar L, Cao Y, Nordlund P. Monitoring Drug Target Engagement in Cells and Tissues Using the Cellular Thermal Shift Assay. Science. 2013; 341:84–87. [PubMed: 23828940]

(19). Tonnesen, HH., editor. Photostability of Drugs and Drug Formulations. 2nd ed.. CRC Press LLC; Boca Raton, FL: 2004. p. 435

(20). Baker SJ, Zhang Y-K, Akama T, Lau A, Zhou H, Hernandez V, Mao W, Alley MRK, Sanders V, Plattner JJ. Discovery of a New Boron-Containing Antifungal Agent, 5-Fluoro-1,3-dihydro-1-

hydroxy-2,1-benzoxaborole (AN2690), for the Potential Treatment of Onychomycosis. J. Med. Chem. 2006; 49:4447–4450. [PubMed: 16854048]

(21). Hecker SJ, Reddy KR, Totrov M, Hirst GC, Lomovskaya O, Griffith DC, King P, Tsivkovski R, Sun D, Sabet M, Tarazi Z, Clifton MC, Atkins K, Raymond A, Potts KT, Abendroth J, Boyer SH, Loutit JS, Morgan EE, Durso S, Dudley MN. Discovery of a Cyclic Boronic Acid β-Lactamase Inhibitor (RPX7009) with Utility vs Class A Serine Carbapenemases. J. Med. Chem. 2015; 58:3682–3692. [PubMed: 25782055]

(22). Adams J. Development of the Proteasome Inhibitor PS-341. Oncologist. 2002; 7:9–16. [PubMed: 11854543]

(23). Dorsey BD, Iqbal M, Chatterjee S, Menta E, Bernardini R, Bernareggi A, Cassarà PG, D'Arasmo G, Ferretti E, De Munari S, Oliva A, Pezzoni G, Allievi C, Strepponi I, Ruggeri B, Ator MA, Williams M, Mallamo JP. Discovery of a Potent, Selective, and Orally Active Proteasome Inhibitor for the Treatment of Cancer. J. Med. Chem. 2008; 51:1068–1072. [PubMed: 18247547]

(24). Hansen MM, Jolly RA, Linder RJ. Boronic Acids and Derivatives—Probing the Structure-Activity Relationships for Mutagenicity. Org. Process Res. Dev. 2015; 19:1507.

(25). O'Donovan MR, Mee CD, Fenner S, Teasdale A, Phillips DH. Boronic acids—A novel class of bacterial mutagen. Mutat. Res., Genet. Toxicol. Environ. Mutagen. 2011; 724:1–6.

(26). Ju K-S, Parales RE. Nitroaromatic Compounds, from Synthesis to Biodegradation. Microbiol. Mol. Biol. Rev. 2010; 74:250–272. [PubMed: 20508249]

(27). Groll M, Berkers CR, Ploegh HL, Ovaa H. Crystal Structure of the Boronic Acid-Based Proteasome Inhibitor Bortezomib in Complex with the Yeast 20S Proteasome. Structure. 2006; 14:451–456. [PubMed: 16531229]

(28). Copeland RA, Basavapathruni A, Moyer M, Scott MP. Impact of enzyme concentration and residence time on apparent activity recovery in jump dilution analysis. Anal. Biochem. 2011; 416:206–210. [PubMed: 21669181]

(29). Chou T-C. Drug Combination Studies and Their Synergy Quantification Using the Chou-Talalay Method. Cancer Res. 2010; 70:440–446. [PubMed: 20068163]

(30). Llona-Minguez S, Desroses M, Ghassemian A, Jacques SA, Eriksson L, Isacksson R, Koolmeister T, Stenmark P, Scobie M, Helleday T. Vinylic MIDA Boronates: New Building Blocks for the Synthesis of Aza-Heterocycles. Chem. - Eur. J. 2015; 21:7394–7398. [PubMed: 25809883]

Europe PMC Funders Author Manuscripts

Europe PMC Funders Author Manuscripts

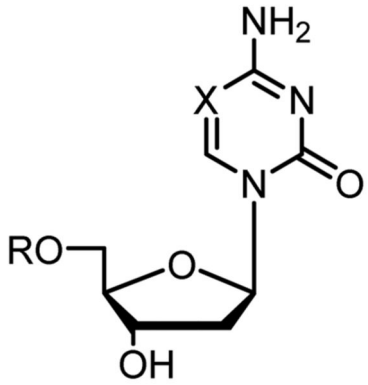

1 X = -CH, R = triphosphate; dCTP

2 X= -N, R = -H; decitabine

3 X= -N, R = triphosphate; 5-aza-dCTP

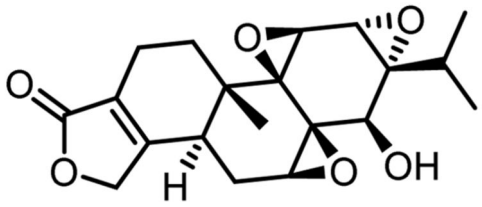

4 triptolide; IC_{50}= 30.9 μM[a]

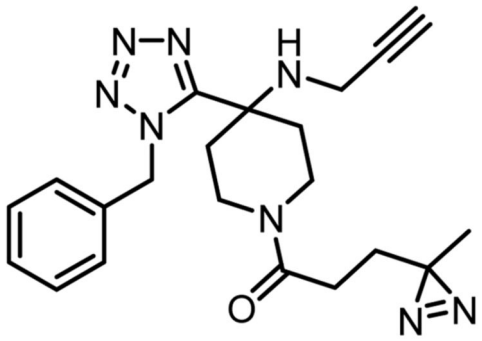

5[b]

Figure 1.
Structures of dCTP, 5-aza-dCTP, and selected dCTPase inhibitors. [a]Using dCTP as the substrate.[1] [b]IC_{50} not available.

Europe PMC Funders Author Manuscripts

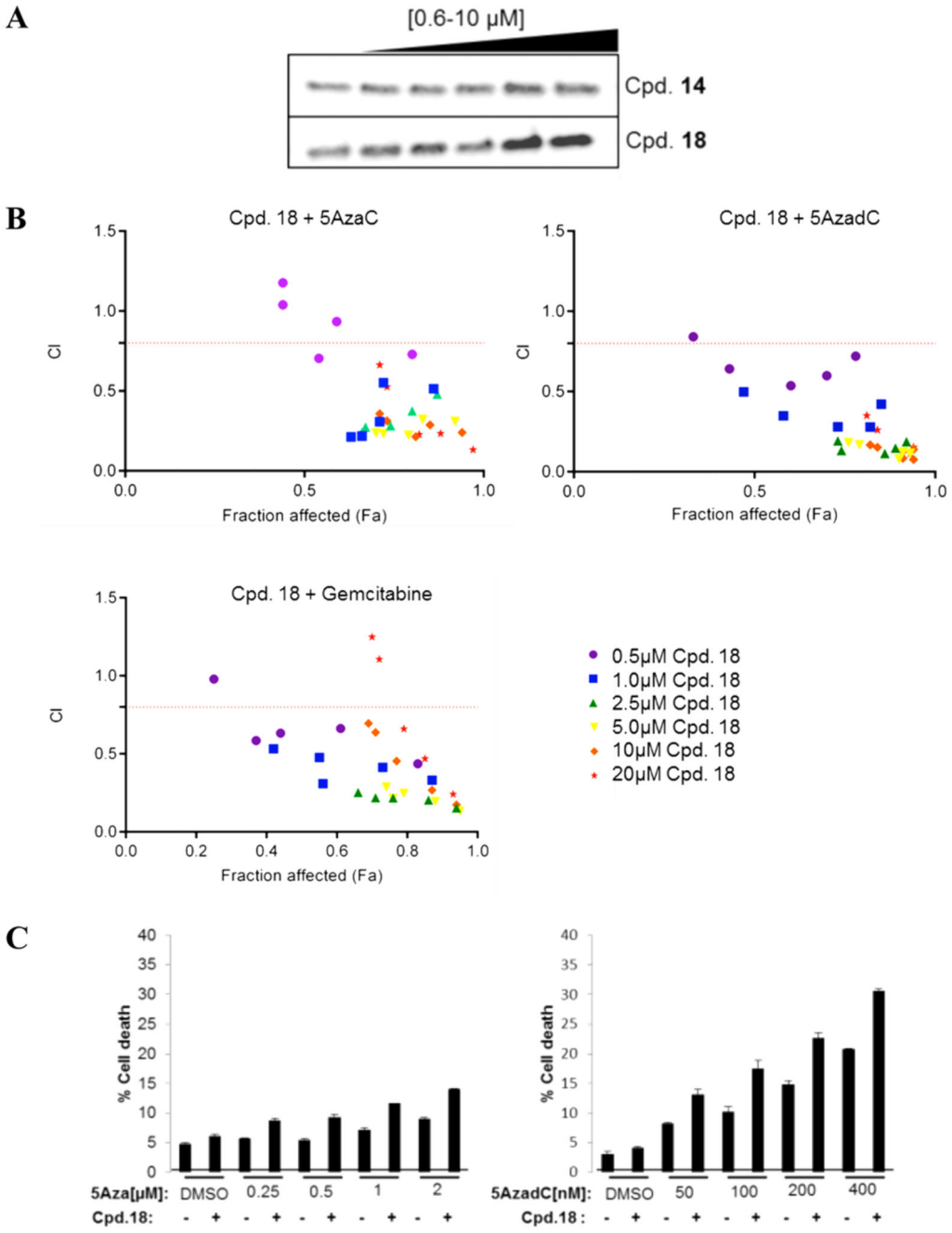

Figure 2.

(A) Western blot images from the cellular thermal shift assay for **14** and **18**. HL60 cells were incubated for 2 h with compounds **14** and **18** (increasing concentrations) and subsequently heated at 67 °C and analyzed for intracellular dCTPase stabilization. (B) Combination index (CI) plots of **18** in combination with cytidine analogues. HL60 cells were incubated for 72 h with different concentrations of compound **18** and cytidine analogues. Cytotoxic effect was determined by Resazurin cell viability assay. (C) Effect of compound **18** in combination with cytidine analogues on cell death. HL60 cells were

incubated for 72 h with compound **18** (2.5 μM) and increasing concentrations of cytidine analogues. Cell death was determined by flow cytometry analysis.

Europe PMC Funders Author Manuscripts

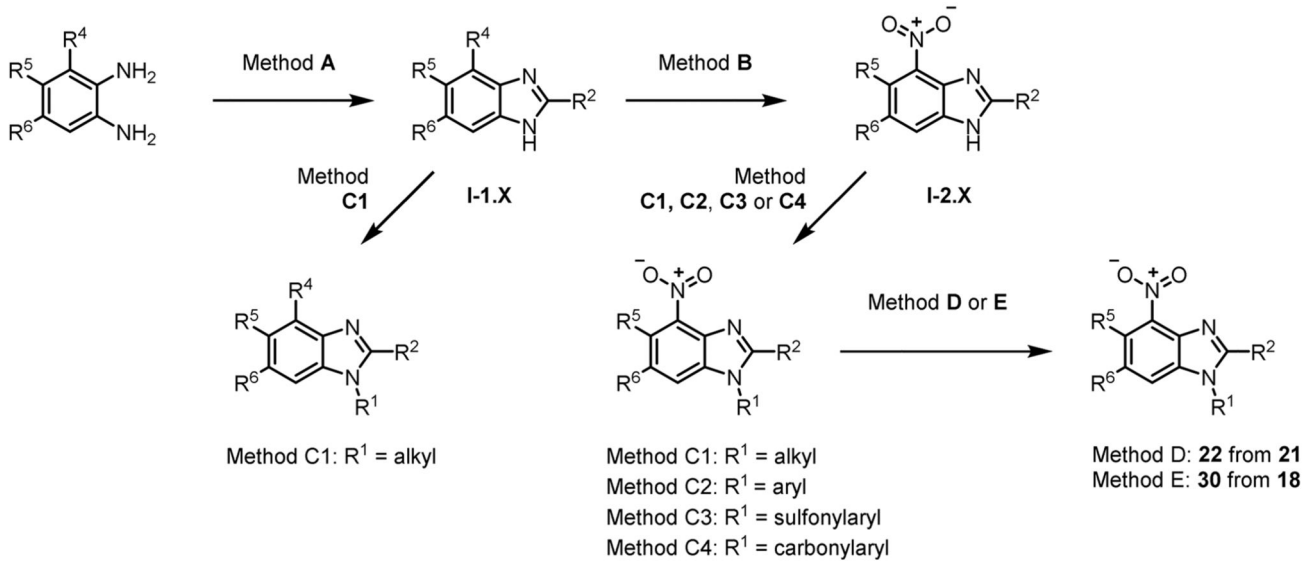

Scheme 1. General Syntheses of Benzimidazole Derivatives[a]

[a]Reagents and conditions: (A) AcOH, 145 °C, 20 min; (B) 65% HNO_3, 95% H_2SO_4, MTBE/MeCN, 0 °C to rt, 16 h; (C1) alkyl halide, K_2CO_3, DMSO, rt, 16 h; (C2) boronic acid, copper acetate, pyridine, DCM, rt, 4 days; (C3) sulfonyl chloride, Et_3N, DCM, rt, 16 h; (C4) acid chloride, Et_3N, DCM, rt, 16 h; (D) 22, LiOH, water/1,4-dioxane, rt, 16 h; (E) 18, *N*-methyliminodiacetic acid, $MgSO_4$, toluene/DMSO, reflux, 1 h.

Table 1
SAR Exploration: 2-, 4-, 5-, and 6-Positions

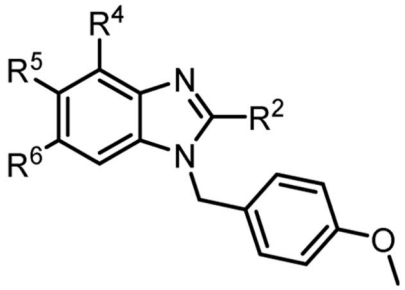

compd	R^2	R^4	R^5/R^6	IC_{50} (μM)
6	Me	NO_2	Me	0.057 ± 0.022[a]
7	H	H	H	>100
8	H	H	Me	>100
9	Me	H	H	>100
10	Me	H	Me	22
11	Me	H	Cl	12
12	Me	NO_2	H	1.45

[a] IC_{50} value determined in three independent runs.

Table 2

SAR Exploration: N1-Position

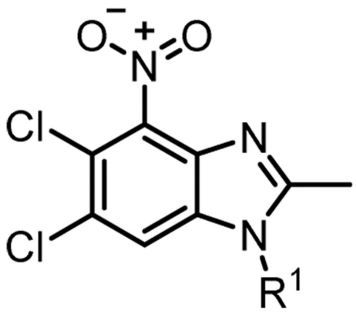

R^1					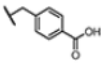
Compd	**13**	**14**	**15**	**16**	**17**
IC$_{50}$ μM	0.049	0.041	0.165	0.019	0.073
R^1	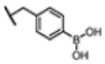			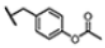	
Compd	**18**	**19**	**20**	**21**	**22**
IC$_{50}$ μM	0.046	0.095	0.133	0.034	0.021
R^1				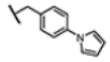	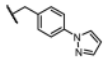
Compd	**23**	**24**	**25**	**26**	**27**
IC$_{50}$ μM	0.240	0.185	0.190	0.331	0.075
R^1			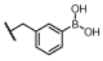	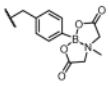	
Compd		**28**	**29**	**30**	
IC$_{50}$ μM		0.082	0.046	0.047	

Table 3

SAR Exploration: N1-Position and Linkers

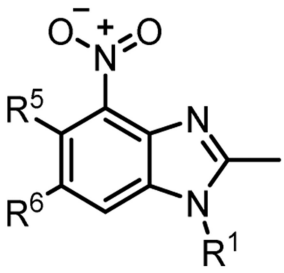

Compd	R^1	R^5/R^6	IC_{50} (μM)
31		−Cl	0.085
32	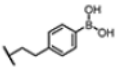	−Cl	0.205
33		−Me	0.250
34		−Cl	0.074
35		−Cl	0.096

Europe PMC Funders Author Manuscripts

Table 4

Additional SAR Exploration: 2-, 4-, 5-, and 6- Positions

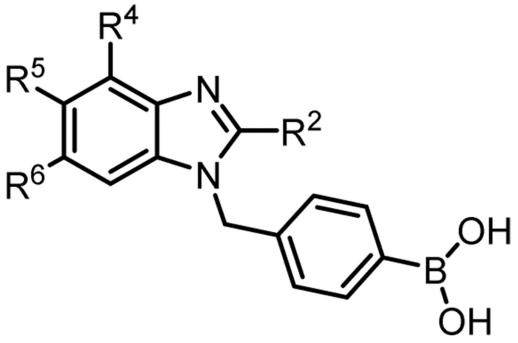

compd	R^2	R^4	R^5/R^6	IC_{50} (μM)
36	cPr	NO_2	Cl	0.027
37	CF_3	NO_2	H	0.206
38	Me	H	Cl	0.248
39	Me	NO_2	F	0.529

Europe PMC Funders Author Manuscripts

Table 5
In Vitro ADME Data for Selected Compounds

	14	22	25	27	36	18	30
$t_{1/2}$ MLM/HLM (min)	8/30	–	7/6	22/38	13/268	197/72	109/11
E MLM/HLM	0.88/0.59	–	0.89/0.83	0.73/0.61	0.83/0.14	0.24/0.38	0.36/0.80
aq solubility (μM)	–	11	–	–	–	52	>100
plasma stability t_{4h} (%)	–	96	–	–	–	11	86
protein binding (F_u %)	–	0.7	–	–	–	0.1	0.8
P_{app} AB/BA (cm/s)	–	–	–	–	–	–	$8.66 \times 10^{-6}/1.30 \times 10^{-3}$
efflux ratio	–	–	–	–	–	–	1.51

Europe PMC Funders Author Manuscripts

Table 6

CYP Inhibition Data for Compound 30

	CYP1A2 (phenacetin)	CYP2C9 (diclofenac)	CYP2C19 (mephenytion)	CYP2D6 (bufuralol)	CYP3A4 (testosterone)	CYP3A4 (midazolam)
IC_{50} (μM)	377.2	1.72	2.93	16.75	21.94	28.12